Korean J. Chem. Eng., 33(5), 1514-1529 (2016)
DOI: 10.1007/s11814-016-0056-z
pISSN: 0256-1115
eISSN: 1975-7220

REVIEW PAPER

Metal hollow sphere electrocatalysts

Jayeeta Chattopadhyay[*,,†], Tara Sankar Pathak[***], Daewon Pak[*], and Rohit Srivastava[****]**

*Graduate School of Energy & Environment, Seoul National University of Science and Technology, Seoul 08826, Korea
**Department of Chemistry, Birla Institute of Technology, Mesra, Deoghar off-campus, Deoghar - 814 142, Jharkhand, India
***Department of Chemistry, Surendra Institute of Engineering and Management, Dhukuria, Siliguri - 734 009, Darjeeling, West Bengal, India
****Department of Inorganic and Physical Chemistry, Indian Institute of Science, Bangalore 560012, India
(*Received 14 July 2015 • accepted 22 February 2016*)

Abstract−Metal micro-/nano hollow spheres have been widely applied in numerous fields during the last decade. This review will only focus on the synthetic strategies to synthesize hollow spherical structures in the enhancement of their electrocatalytic activity, especially the metal hollow spherical materials. We present a comprehensive overview of synthetic strategies for metal hollow spherical structures which have been approached specifically in electrochemical reactions. These synthetic methods are mainly categorized as hard templates, soft templates, sacrificial templates and without templates. The review further includes electrocatalytic approaches of hollow spherical metals in different electrochemical processes, especially the methanol electro-oxidation reaction for methanol fuel cell application and hydrogen and oxygen evolution reactions in water electrolyzer, as metal hollow spherical materials are especially applied in these specific reactions.

Keywords: Metal Hollow Sphere, Synthesis, Electrocatalysts, Methanol Electro-oxidation, Water Electrolyzer

INTRODUCTION

Hollow spherical structures have attracted huge interest as a special class of materials in comparison to other solid counterparts, owing to their higher surface area, lower density, better permeation and physical and thermal stability [1-5]. In a growing number of applications, such as catalysis, drug and gene delivery, cosmetics, hydrogen production and storage, chemical reactors, sensors, photonics, photovoltaics, rechargeable batteries, and electrocatalysis, the chemical growth and distribution of matter within the particles play pivotal roles in function determinations [6-15]. Titania multi-shell hollow micro-structures are used in Li ion batteries for their excellent rate capacity, good cycling performance and high specific capacity [16]. Xu et al. reported α-Fe_2O_3 multi-shell hollow microspheres as lithium ion battery anodes with superior capacity and charge retention [17]. Multi-shelled Co_3O_4 microspheres have also been used for the same purpose by Wang et al. [18]. Triple shelled CeO_2 spheres have also been used as photocatalyst in water oxidation, and shown excellent activity and enormous stability for O_2 evolution [19]. Au@TiO_2 core-shell hollow spheres have been used as dye-sensitized solar cells with remarkable efficiency [20]. Similarly, quintuple-shelled SnO_2 hollow microspheres have also been applied in dye-sensitized solar cells by Dong et al. [21]. Ni and Ni/Pt hollow nanospheres have been applied as catalyst in hydrolysis of ammonia borane [22]. The same research group synthesized nanoscale multi-shell Au/CeO_2 hollow spheres also [23]. Similar work has been reported by Xu et al. about Pt and Pd nanotubular materials with application in fuel cell technology [24]. In all the cases, the large void space created inside the spherical structure can be successfully utilized to encapsulate and release sensitive materials [25,26]. Hybrid materials are actually the combinations of organic and inorganic building blocks, uniformly distributed in the framework, attracting attention due to the combination of the functional versatility of organic chemistry with the advantages of thermal stability of inorganic substrates [27,28]. It is very important to control morphology of the organic-inorganic hybrid materials in order to utilize them in desired applications [28-30]. There are various methods, such as templating [31-33], sono-chemical [34,35], hydrothermal [36-38] and so on, which have been reported as the preparation procedures for the inorganic materials with hollow spherical structures. The use of templates to fabricate such hollow spherical structure of inorganic materials has proven very successful. Yang et al. proposed a typical way of Pt hollow nanosphere synthesis with bis(p-sulfonatophenyl)phenylphosphine [39]. Guo et al. similarly reported another way of urchin-like morphology though sacrificial template method [40]. Chen et al. worked on platinum hollow spheres with nano-channels, which have been utilized as an active catalyst in oxygen reduction [41]. Silver nanoparticles have been used as the sacrificial template in this process, and incomplete shell with presence of multi nano-channels on all over the spheres actually enhanced the catalytic activity of this material. Liu et al. reported the synthetic procedure of cage-ball structured of Pt-Ru nanoparticles with their outstanding methanol tolerance during cathode reaction of direct metha-

†To whom correspondence should be addressed.
E-mail: jayeeta08@gmail.com

nol fuel cell (DMFC) [42]. The cage-ball structure actually resulted in the differential diffusion of methanol and oxygen during the process. Another research group reported a cost-effective synthetic approach of carbon supported Pt-containing noble metal nanoparticles with hollow interior [43]. In this work, Pt-containing core-shell Ag-noble metal nanoparticles hollowed by NaCl on carbon support exhibited enhancement in the catalytic activity for methanol oxidation reaction. A variety of sacrificial templates, including polystyrene latex particles or silica particles [44-49] and their crystalline array [50], emulsion [51], polymer - surfactant complex micelles [52], polymer aggregates [53] and vesicles [54], were developed. It is seen that, spray pyrolysis method is not suitable for hollow morphology due to the low density and low strength. Extensive researches were performed to maintain the hollow or fractured structures of the materials, which is actually based on the understanding of physical and chemical happening in a single - droplet [55-58]. Wang et al. proposed a synthetic method for Pt-Pd bimetallic nanoparticles, which has been termed as "metallic nanocages" with a hollow interior and porous dendritic shell. This synthesis was achieved by selective chemical etching of Pd cores from dendritic Pt-on-Pd nanoparticles. The obtained Pt-Pd nanocages show superior catalytic activity for methanol oxidation reaction [59]. Hollow particles have been synthesized using aerosol process under the different conditions of fast evaporation, lower supersaturation, surface reaction, low permeability of crust, lower temperature of reactor, and shorter residence time [60,61].

Lou et al. [62] already reported an extensive review on the synthesis and applications of hollow micro and nanostructures. Qi et al. also reviewed multi-shell hollow micro/-nanostructure materials with their different synthetic methodologies as well as their compositional and geometric manipulation with their applications in energy conversion and storage, sensors, photocatalysis, and drug delivery [63]. The present review only focuses on the synthetic strategies to synthesize hollow spherical structures in the enhancement of their electrocatalytic activity, especially the metal hollow spherical materials. As we all know, electrochemical technology is playing an increasingly important role in modern society and especially in the chemical industry [64]. One of the major reasons for the shift in interest towards electrochemical technology is the need for clean and efficient energy sources, especially for transport systems [65-67]. Fuel cells are considered as efficient and non-polluting power sources offering much higher energy density and energy efficiency in comparison to other conventional systems. A fuel cell is an 'electrochemical' device that converts the chemical energy of a fuel (e.g., hydrogen, methanol) and an oxidant (air or pure oxygen) in the presence of a catalyst into electricity, heat and water. Similarly, water electrolysis represents the most important process to produce hydrogen without evolution of CO_2. It is overviewed that very few researchers have explored the special electrocatalytic properties of metal hollow spheres, whereas this particular research area can be emphasized more in the present scenario of scarcity in hydrocarbon fuels. Most of the research groups have reported the electrocatalytic approach of metal loaded over hollow carbon spheres, but metal hollow spheres have always been neglected to be explored in this way. Moreover, this carbon is known to undergo electrochemical oxidation under a fuel cell operating environment, specifically at potentials above 0.9 V, leading to a loss of electrocatalysts and formation of CO_2 during fuel cell performance. Thus, it is important to explore non-carbon hollow spherical materials as electrocatalysts in different fuel cell and water electrolyzer systems [68]. It is reviewed from the literature that, metal hollow sphere electrocatalysts have specifically been utilized in polymer electrolyte membrane fuel cells (PEMFC) for oxygen reduction [69], methanol electro-oxidation for direct methanol fuel cells (DMFC), supercapacitor electrodes [70] and also in the water electrolysis technology for hydrogen and oxygen production. In the first section of the review, primary synthetic techniques to produce hollow spherical materials are presented. The next part emphasizes the electrocatalytic aspects of them in different electrochemical technologies.

STRATEGY TO SYNTHESIZE HOLLOW STRUCTURES

The materials with hollow spherical structures usually possess greater electrocatalytic activity due to their large void space inside the sphere, with the formation of numerous pores all over the spherical structure, which actually increases the surface area of the materials with greater adsorption characteristics of the products in a specific electrochemical reaction. We can divide various synthetic approaches, which have been utilized to synthesize metal hollow spherical electrocatalysts into these categories: (a) conventional templating synthesis (b) sacrificial templating synthesis (c) without-templating synthesis.

1. Preparation of Hollow Spheres Using Templates

1-1. Hard Templates

Synthesis of hollow spherical structures using templates involves four major steps, which are illustrated in the schematic diagram

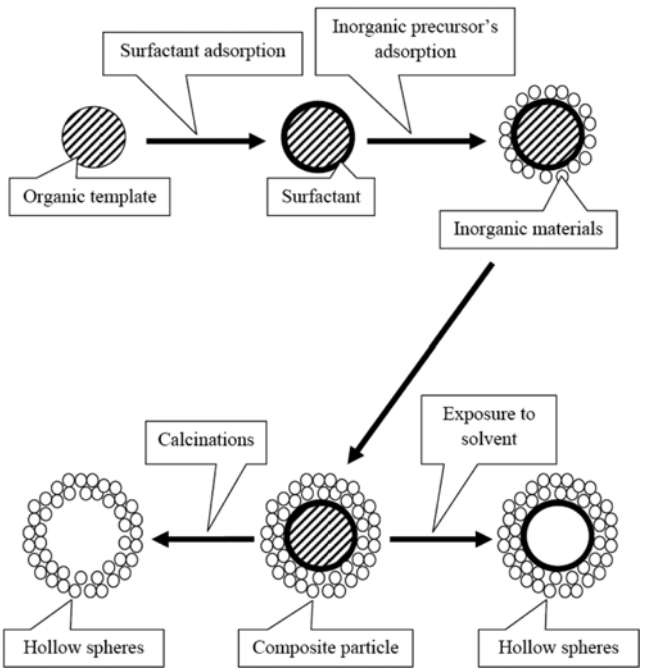

Fig. 1. Schematic diagram of procedure to synthesize hollow spherical materials using templating method.

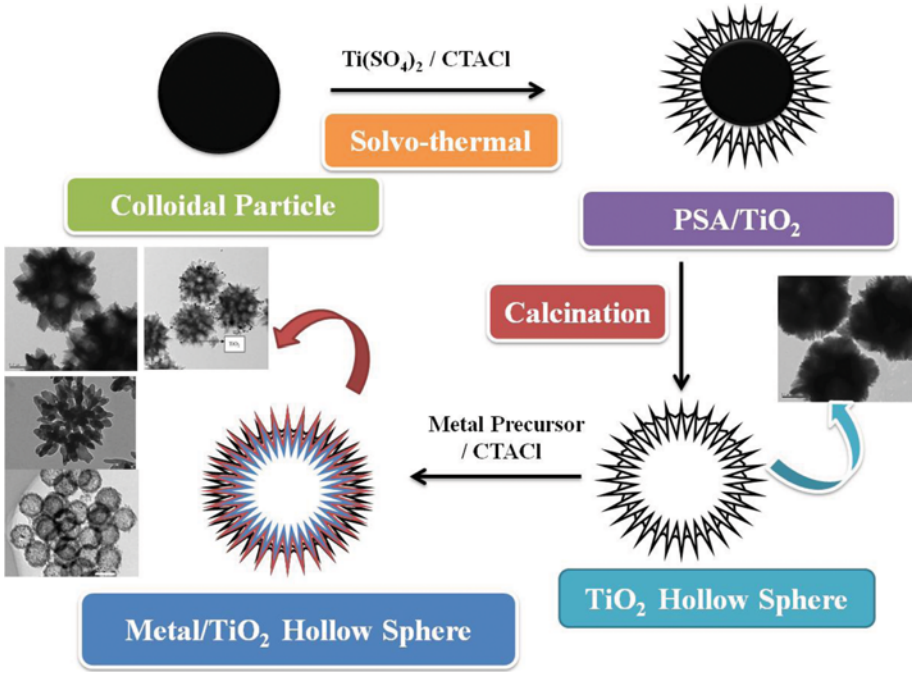

Fig. 2. Schematic diagram of titania hollow sphere synthesis using PSA latex as core material.

presented in Fig. 1. At first, hard template synthesis, which is followed by the modification of template surface to achieve favorable surface properties. The modified templates are then coated by the designed materials or their precursors to achieve compact shells. The final step typically entails selective etching of the template in appropriate solvents or calcination at high temperatures. In either approach, one should be cautious to prevent collapsing of the shells during template removal. Sometimes, during dissolving of template materials with the application of organic solvent, swelling of the polymer can rapture the hollow sphere structure.

The layer-by-layer assembly synthesis method is included in the hard templating procedure. In this process, oppositely charged polymer species are sequentially deposited on substrate by electrostatic interactions. Caruso et al. [41] at first applied this method with the combination of colloidal templating to synthesize hollow silica and hybrid capsules with the electrostatic interaction of negatively charged silica particles and positively charged polymer PDADMAC {poly (diallyldimethylammonium chloride)}. In this process, the assembly process can be repeated to form a multi-layer structure with considerable wall thickness. Polymer capsules: this method permits major control over capsule properties, e.g. size, composition, thickness, permeability, functions with the choice of the sacrificial colloids and the coating components. Although, it is very difficult to synthesize smaller hollow structures with sizes <200 nm using this tedious method and no research group has yet reported this synthetic approach in metal hollow sphere preparation with electrocatalytic applications.

A simpler synthetic approach with easy-to-control over particle size can be achieved with the sol-gel method. It is often employed for the coating of colloidal templates with the formation of hollow spherical structures, and templates are further removed by calcination or with the exposure to solvent. The formation of silica and titania hollow sphere is mostly reported in the literature using poly(styrene) (PS) or poly(styrene-methacrylic acid) (PSA) latex as core materials and silica or titania as the shell [71-77]. Fig. 2 presents a schematic diagram of titania hollow sphere synthesis using PSA as core material. Imhof et al. reported a one-step method to cover cationic polystyrene spheres with titania precipitated during the hydrolysis of a titania alkoxide [78,88]. Similarly, titania-polystyrene composite particles were formed by Li et al., as titanium tetrabutoxide hydrolyzed around polystyrene particles into amorphous titania as a result of its exposure to the moisture present in the air atmosphere [79]. Wang et al. at first successfully prepared titania hollow spheres using titania sulfate ($Ti(SO_4)_2$) as the precursor material instead of organometallic titanium [80]. They deposited inorganic coatings over the PSA latex particles, which acted as the core material. A similar synthetic approach was reported by Kim et al. [81] and Chattopadhyay et al. [82]. This group first mentioned the utilization of metal-doped titania hollow spherical materials as electrocatalysts in hydrogen and oxygen production from water electrolysis. In this work, they required void interior space of the hollow spheres, inside which adsorbed hydrogen and oxygen could be captured. Therefore, they added cetyltrimethylammonium chloride (CTACl) as surfactant, which formed radially oriented micro- or meso-channels throughout the surface, resulting in the greater electrocatalytic activity of the titania hollow spheres. In this method, titania sulfate is added into water under vigorous stirring, followed by the addition of PSA latex, HCl and CTACl. The mixture was kept ageing for 12 h at 70 °C, cooled to ambient temperature, centrifuged, washed with water and ethanol, and dried at 60 °C for 12 h, finally resulting in the formation of titania hollow spheres. Further, the metal doping over titania hollow spheres was achieved with similar deposition process using sol-gel method applying corresponding metal precursors. The core

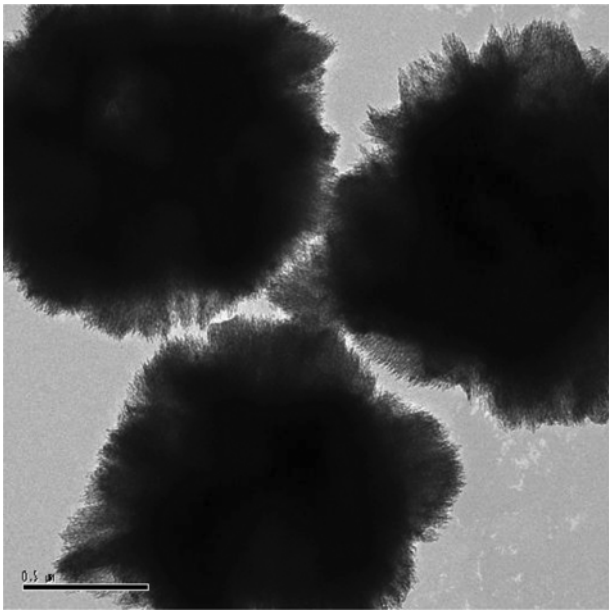

Fig. 3. TEM image of pure TiO_2 hollow spheres [82].

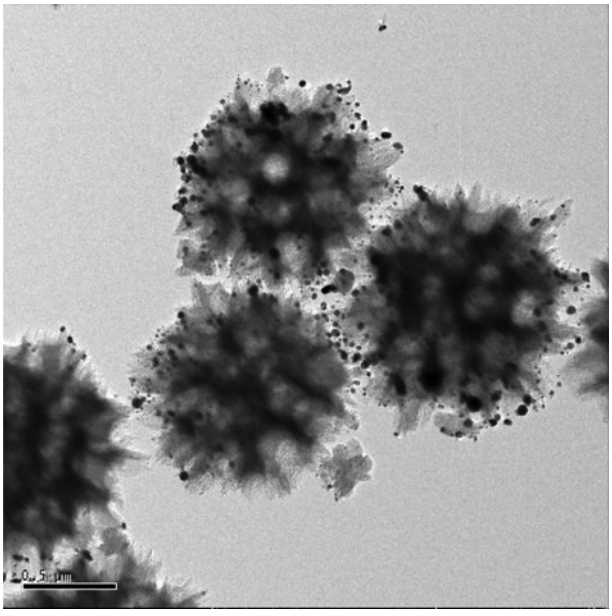

Fig. 4. TEM image of 20 wt% Pt/TiO_2 hollow spheres [81].

material was further removed by the calcination process. The formation of rutile TiO_2 phase was confirmed by the XRD studies, whereas SEM and TEM images showed remarkable covering of doping metal all over the titania spheres. Fig. 3 presents the TEM image of pure TiO_2 hollow spherical materials calcined with 300 °C with the particle size of 1-1.2 μm. Initially, this group worked on Pt-doped titania hollow sphere electrocatalysts and later tried to utilize less expensive semi-conducting metals (tin and barium) as dopant to replace the platinum [82,83]. The TEM image of 20 wt% Pt-doped titania materials (Fig. 4) clearly shows the porous structure with the hollow core space with size ranging from 900 to 1,000 nm, with the platinum particle size of 5 to 70 nm [81].

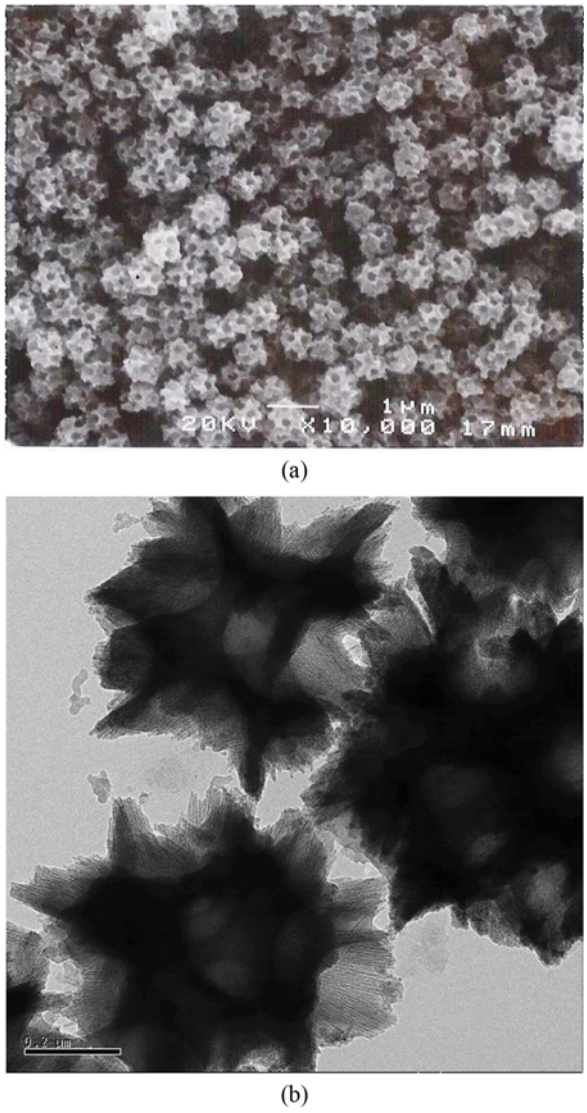

Fig. 5. (a) And (b): SEM and TEM images of 40 wt% Sn-doped titania hollow sphere electrocatalysts calcined at 300 °C [82].

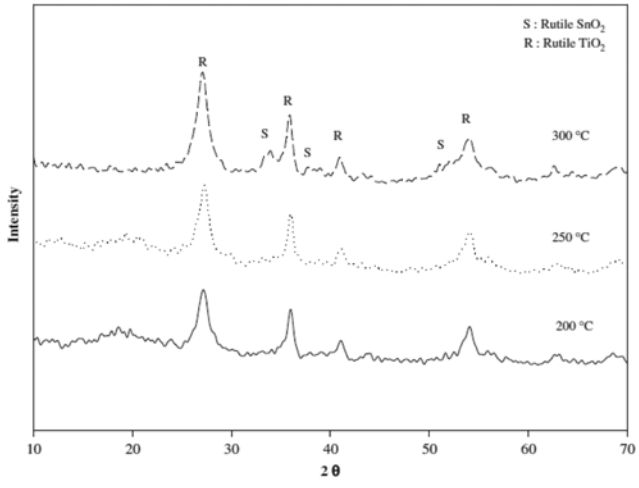

Fig. 6. XRD patterns of 40 wt% Sn-doped TiO_2 hollow spheres calcined at 200, 250, and 300 °C [82].

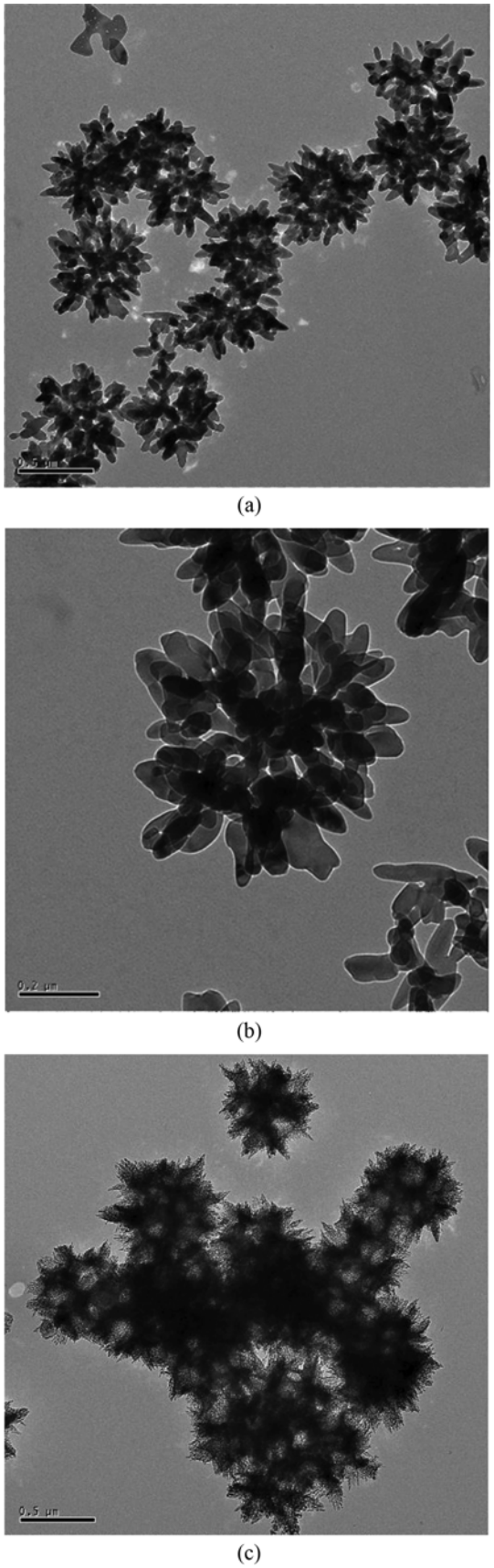

Fig. 7. TEM images of (a) and (b) 40 wt% Ba/TiO_2 calcined at 500 °C and (c) calcined at 700 °C [83].

Using $SnCl_2 \cdot 2HCl$ as the precursor, tin was doped over the spheres, the size of the Sn/TiO_2 was shrunk to some extent during heat treatment, resulting in hollow spheres with the average diameter of 0.4-0.6 μm with uniform layer of SnO_2 over the titania spheres (Fig. 5) [82]. The diffraction peaks in XRD patterns (Fig. 6) confirmed the formation of rutile SnO_2 and TiO_2 phases in Sn/TiO_2 hollow spheres. Critical growth of both the phases was found with increase in the calcination temperatures. Later, Son et al. did similar work on barium doped titania hollow sphere electrocatalysts [83].

Ba/TiO_2 hollow spheres were also synthesized with the average diameter of 0.4-0.5 μm, irrespective of the change in the calcination temperatures of the electrocatalysts with the uniform covering of barium all over the spherical surface. Although, the surface of the spheres started cracking with increase in the calcination temperature, resulting in the incorporation of barium through the cracks inside the spheres for the electrocatalysts calcined at 700 °C (Fig. 7) [83]. Similarly, Ni-doped titania hollow spheres were reported as electrocatalysts both in aqueous [84] and polymer electrolyte membrane (PEM) water electrolyzer [85]. These materials contained the uniform layer of nickel nanoparticles (10-65 nm) over the spherical structure, with the average sphere diameter of 0.8-0.9 μm with the presence of NiO and rutile TiO_2 phase on the catalyst surface; their presence was also confirmed from XRD studies (Fig. 8). Fig. 9(a) and (b) show TEM images of Ni-doped titania hollow spheres [84], whereas 9(c) presents the SEM of Ni/TiO_2 hollow sphere materials [85]. In all the cases, the catalyst concentration was 0.1 mol L^{-1}. All these metal doped hollow sphere electrocatalysts of high surface area were performed with great potential in the hydrogen and oxygen evolution reaction in acidic media, as rutile TiO_2 phase is very stable in acid. The electrocatalytic studies of these materials will be discussed later.

1-2. Soft Templates

Hard templating is the most convenient, effective and common method in preparation of hollow spherical material, although lack of robustness with the multistep synthetic process has shifted the synthetic approach towards soft templating process. This process includes structures formed by emulsion droplets, surfactants, long-chain polymers, and viruses, which are usually amphiphilic molecules containing a hydrophilic head and a hydrophobic chain [86].

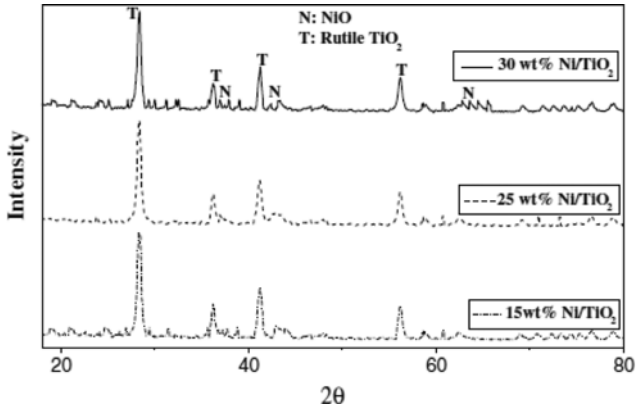

Fig. 8. XRD patterns of 15, 25 and 30 wt% Ni-doped TiO_2 hollow spheres calcined at 400 °C.

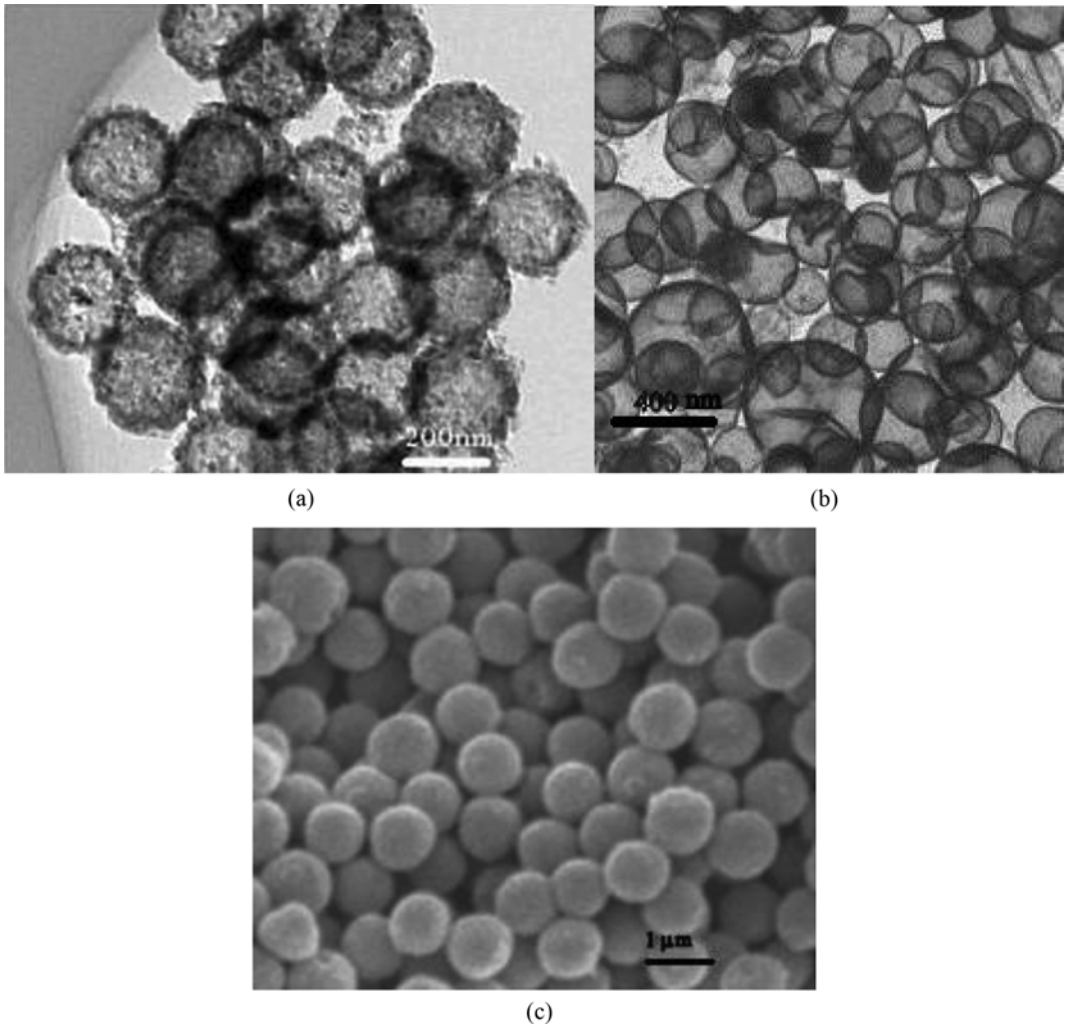

Fig. 9. (a) and (b): TEM images of Ni/TiO_2 hollow spheres; [84] (c) SEM image of Ni/TiO_2 hollow spheres [85].

Sol-gel processes for metal alkoxides are usually employed in emulsion templating to prepare titania and silica [86-90]. Nakashima et al. reported preparation of 3-20 μm sized titania hollow spheres by templating against toluene microdroplets in 1-butyl-3-methylimidazolium hexafluorophosphate ionic liquid [91]. Although, no research group has yet reported this synthetic approach to get hollow spheres with electrocatalytic activity as their application. However, the relatively low stability and the poly-dispersity of soft templates may limit their application as electrocatalysts. Moreover, soft templating is often limited by the difficulty in controlling the uniformity of the products.

1-3. Sacrificial Templates

A sacrificial template is defined as a template which itself is involved as a reactant in the synthetic method of the shell or its intermediate. In this process, the sacrificial template is partially or completely consumed during the synthesis process. It directly determines the shape and cavity size of the resultant hollow sphere materials. Thus, this method does not apply any additional surface functionalization, and shell formation process can be confirmed from the chemical reaction. Mainly, Kirkendall effect and galvanic replacement techniques have become most popular in sacrificial templating synthetic approach. Guo et al. synthesized sponge-like Au/Pt/core/shell nanostructured materials via a simple two-step wet chemical process, which acted as electrocatalysts in oxygen reduction reaction and methanol oxidation [92]. In Au/Pt nanomaterial synthesis, gold hollow spheres were synthesized using the galvanic displacement reactions with Co nanoparticles and $HAuCl_4$. In the galvanic replacement reaction, the driving force comes from the large reduction potential gap initiated between $AuCl_4^-$/Au and Co^{2+}/Co redox couples. The cobalt nanoparticles were formed by the reduction of Co^{2+} with $NaBH_4$ employing the galvanic replacement reactions [93].

$$3Co+2AuCl_4^- \rightarrow 2Au+3Co^{2+}+8Cl^-$$

These gold nanospheres with hollow structures were further used as seeds to grow sponge-like Pt shells by the successive reduction of the chloroplatinic acid with ascorbic acid. Similarly, Qu et al. subsequently prepared Au-Ag-Pt core-shell-shell and hollow Pt nanoparticles with enhanced electrocatalytic activity toward oxygen reduction reaction performed in PEMFC [94]. They initially synthesized Au and Ag seed nanoparticles with $NaBH_4$ reduction of $HAuCl_4$ and $AgNO_3$. They also followed the successive reduc-

tion method, also known as the seed mediated method, to synthesize the Au-Ag (core-shell) and Au-Ag-Pt (core-shell-shell) hollow spherical nanomaterials employing aqueous sodium citrate as reducing agent. The hollow Pt nanoparticles were obtained using Ag as core material with the successive reduction process. Guo et al. reported the synthesis of PtCo nanosphere electrocatalysts supported on multi-walled carbon nanotubes, which were employed in methanol electrooxidation [95]. They also followed the successive reduction method using $NaBH_4$ as the reducing agent of $CoCl_2$ and H_2PtCl_6, followed by the addition of multi-walled CNTs in the reaction mixture. The same research group had synthesized hollow and solid PtRu nanosphere electrocatalysts supported on MWCNTs employing cobalt nanoparticles as sacrificial templates [96]. Electrocatalytic activity in methanol electrooxidation was exhibited in these materials, with successive comparison with commercial PtRu/C electrocatalyst. Wei et al. investigated carbon-supported Au hollow nanospheres with electrocatalytic activity in BH_4^- electrooxidation [97]. Au hollow nanoparticles were formed using cobalt nanoparticles as sacrificial template using galvanic replacement method [92]. Finally the hollow Au nanospheres were dispersed on Vulcan XC-72R carbon. They also made solid nanoparticles of gold using citrate reduction method [98], comparing their successive electrocatalytic activity in electrooxidation reaction of BH_4^-.

Xu et al. synthesized Ni hollow spherical electrocatalysts consisting of needle-like nickel particles using silica spheres as template with gold nanoparticles seeding method [99]. Their electrocatalytic activities were examined for methanol and ethanol electrooxidation reaction for direct alcohol fuel cells and in alcohol sensors. They at first applied ammonia and 3-aminopropyltrimethoxysilane (APTMS) on silica spheres to achieve amine moieties coatings on the surface of the silica [100,101]. The gold nanoparticles were further introduced with APTMS-functionalized silica spheres employing successive reduction method, which resulted in the formation of silica spheres with well separated gold nanoparticles on the surface. These were then added into $NiCl_2$ ethylene glycol solution followed by the addition of hydrazine for further reduction, finally achieving silica-nickel core-shell material. Silica core was then dissolved with NaOH solvation method.

The Kirkendall effect is another popular way to synthesize materials with void formation near interfaces with the application of different inter-diffusion rates in bulk diffusion couple [102]. The net flow of mass in one direction is balanced by a flux of vacancies, which then condense into voids preferably around the interface. This synthetic approach becomes more complicated during the spherical structure formation due to their dominant roles of curvature and surface energetic [103]. Yin et al. first explained the formation of cobalt oxide hollow nanocrystals and chalcogenides with 10-20 nm size [104]. The pre-synthesized Co nanocrystals were reacted with sulfur; during the sulfidation process they were covered with a very thin layer of cobalt sulfide. In the further growth of CoS shell, diffusion of single dominant species is required, and in the present system, outward diffusion of Co happened, resulting in the formation of single void in each nanoparticle. Dubau et al. approached this synthetic process to form Pt_3CoC electrocatalysts in oxygen reduction reaction for PEMFC, with formation of hollow Pt nanoparticles [105]. They got the evidence that Co atoms containing Pt_3Co/C nanoparticles segregate to the surface for long-term operation in PEMFC [106-108].

The inverted colloidal crystal template technique is exhibited in the preparation of 3D ordered macroporous gold film [109,110], Pt [111], Pt/Ru nanocomposites [112] Polyanniline (PANI) [113] and palladium hollow spheres [114], having wide applications in electrocatalysis, immunoassay [109,113] and direct alcohol fuel cells (DAFCs) [111,112]. Dai et al. reported the fabrication of palladium hollow sphere array with the same synthetic approach, which has been applied as electrocatalysts in direct electro-oxidation of ethanol in alkaline media for DAFCs [114]. At first, a close-packed silica colloidal crystal layer was formed on the gold substrate with vertical deposition technique. Further, Pd was electrodeposited on the silica spheres with immersing the electrode in Poly (Diallyl Dimethyl Ammonium Chloride) (PDDA) and $PdCl_2$ solution, and finally silica core was removed by applying HF solution.

2. Preparation of Hollow Spheres without Using Templates

The difficulties faced during synthesis of hollow sphere with templating methods have attracted researchers' attention towards template-free methods. In hard templating, the template removal method significantly complicates the process and affects the quality of the materials. Among various template-free methods, Ostwald ripening is the most popular one in which growth of large precipitates at the expense of smaller precipitates caused by energetic factors [115]. The solution-spray plasma (SSP) method is another simple one-step preparation technique. The SSP apparatus consists of an ultrasonic mist generator with a plasma torch reactor and a catalyst particle collector with a water shower supplied by a circulatory pump [116]. Nishida et al. prepared nickel nanoparticles on hollow samaria-doped ceria (SDC) particles via this SSP technique, which were used as anode catalysts for solid oxide fuel cells (SOFCs) [117]. They prepared a mixed solution of cerium and samarium nitrates with atomic ratio of 80 : 20; nickel nitrate was added subsequently according to the loading percentage. After forming the plasma torch, a mist of mixed solution was formed in the carrier gas (Ar and O_2) using ultrasonic atomizer. The mist formed in the plasma then decomposed to get mixed oxide of Ni and SDC. In another template-free synthesis method, Li et al. reported the deposition of Pd nanoparticles on Fe_3O_4 hollow nanospheres, in which Fe_3O_4 hollow spheres were synthesized using solvothermal technique [118]. The homogeneous ethylene glycol solution of ferric chloride was sealed in a PTEE-lined stainless steel autoclave at 180 °C for 20 h, and black precipitate was formed, which was then further washed and dried in vacuum. Further, $PdCl_2$ solution was mixed with this black material under reduction of $NaBH_4$ with vigorous stirring, and Pd-loaded Fe_3O_4 hollow nanospheres were synthesized, which were further utilized as electrocatalyst in electrooxidation of methanol in alkaline media. Hu et al. synthesized Pt-Ni nanospheres using successive reduction of $NiCl_2$ and K_2PtCl_6 solution employing $NaBH_4$ as reducing agent with continuous stirring; PVP was used as the capping ligand [119]. The resultant material was collected after centrifugation, washed sequentially with double distilled water (DDW), and dried at vacuum at ambient temperature. These were further loaded with Vulcan XC-72 carbon with chemical deposition method. In the

Table 1. Metal Spherical Structures of various synthetic approaches with different electrocatalytic activity in literature

Sl. No.	Materials	Application	Synthetic approach	References
1	Pt doped on TiO_2 hollow sphere	Water electrolysis	Hard templates	Kim et al. [81]
2	Sn doped on TiO_2 hollow sphere	Water Electrolysis	Hard templates	Chattopadhyay et al. [82]
3	Ba doped on TiO_2 hollow sphere	Water Electrolysis	Hard templates	Son et al. [83]
4	Ni dopen on TiO_2 hollow sphere	Water Electrolysis	Hard templates	Chattopadhyay et al. [84]
5	Ni doped on TiO_2 hollow sphere	PEM Electrolyzer	Hard templates	Chattopadhyay et al. [85]
6	Au/Pt/core/shell nano-spheres	ORR and methanol oxidation	Sacrificial templates (Wet chemical process)	Guo et al. [92]
7	Au-Ag-Pt core-shell-shell spheres	ORR in PEMFC	Sacrificial templates (Seed mediated method)	Qu et al. [94]
8	PtCo nanospheres on MWCNTs	Methanol electrooxidation	Sacrificial templates	Guo et al. [95]
9	PtRu nanospheres on MWCNTs	Methanol electrooxidation	Sacrificial templates	Guo et al. [96]
10	Carbon supported Au hollow nanospheres	BH_4^- electrooxidation	Sacrificial templates	Wei et al. [97]
11	Ni hollow spheres	Methanol and ethanol electrooxidation for DAFCs and in alcohol sensors	Sacrificial templates (Seed mediated method)	Xu et al. [99]
12	Pt_3CoC with hollow Pt nanoparticles	ORR in PEMFC	Sacrificial templates	Dabau et al. [106]
13	Nickel nanoparticles on hollow Samaria-doped ceria particles	Anode catalysts in SOFCs	Solution-spray plasma (SSP) method	Nishida et al. [117]
14	Pd nanoparticles on Fe_3O_4 hollow spheres	Methanol electrooxidation in alkaline media	Solvothermal method	Li et al. [118]
15	Pt-Ni nanopsheres	Methanol electrooxidation	Successive reduction method	Hu et al. [119]
16	PtNi hollow nanospheres	Methanol electrooxidation	Successive reduction method	Zhou et al. [120]
17	Co-Pt hollow spheres	Methanol electrooxidation	One-step chemical synthesis method	Chen et al. [121]

same way, Zhou et al. prepared PtNi hollow nanospheres with successive reduction process with $NaBH_4$ [120]. Both research groups utilized the hollow sphere electrocatalysts for methanol electrooxidation purpose. Chen et al. reported the successful one-step chemical synthesis of Co-Pt hollow sphere electrocatalysts [121]. In a typical synthesis procedure, platinum acetylacetonate and sodium dodecyl sulfate (SDS) were dissolved in ethylene glycol solvent. They maintained the reflux temperature of the reaction mixture at 198 °C in a three-neck flask until the black color precipitate was formed. It was collected, washed with DDW and dried at ambient conditions. They also synthesized Pt nanoparticles using similar conditions, except the addition of precursor of cobalt, to compare their electrocatalytic activity in methanol electrooxidation reaction.

ELECTROCATALYTIC APPLICATIONS OF METAL SPHERES

1. Metal Sphere Electrocatalysts in Methanol Electrooxidation Reaction

The electrocatalysis of methanol oxidation reaction is the most difficult task in the realization of a direct methanol fuel cell (DMFC) [122,123]. The methanol oxidation reaction produces CO_2. The thermodynamic potential value of this reaction is very close to equilibrium potential of hydrogen, although the methanol oxidation reaction is much slower than the hydrogen counterpart.

$$CH_3OH + H_2O \rightarrow CO_2 + 6H^+ + 6e^- \qquad E^o = 0.02\ V$$

The mechanism of this reaction consists of two different mechanisms, both of them present as parallel reactions. In both of the pathways, catalysts should be involved to break the C-H bond and proceed the reaction with some O-containing species, which are joined with the previous resulting residue to produce CO_2 or HCOOH. The schematic diagram (Fig. 10) explains the detailed mechanism of methanol oxidation. During the methanol adsorption process, the methanol molecules will seek several neighbor-

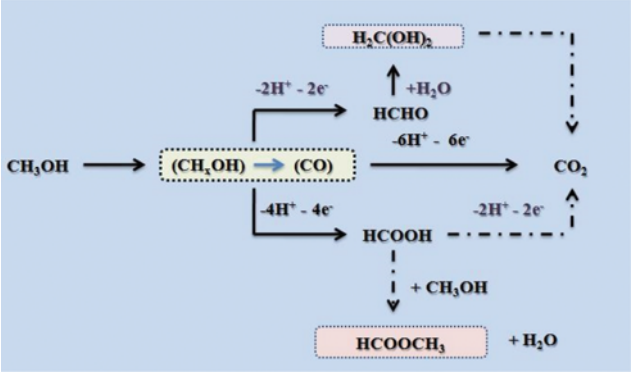

Fig. 10. Schematic diagram of methanol oxidation mechanism.

ing places on the electrode surface; as methanol cannot displace the adsorbed H atoms, therefore adsorption can only happen where enough numbers of Pt sites become free from H [124]. If a cyclic voltammogram is initiated after contracting a polycrystalline Pt electrode with a methanol containing solution at a potential of 0.05 V or less, methanol adsorption phenomena will happen as soon as hydrogen coverage decreases to a certain extent [125].

Many groups have emphasized on the nano-hollow sphere electrocatalysts in methanol electro-oxidation reaction. Chen et al. considered CoPt hollow spheres as electrocatalysts for this purpose. They had compared their cyclic voltammogram results with those of Pt and CoPt nanoparticles synthesized by them [121]. The experiments were in a 0.5 M H_2SO_4 aqueous solution and 0.5 M H_2SO_4 aqueous solution and 1 M methanol solution. According to their results, the current densities in the hydrogen adsorption/desorption and oxide formation/regions of the hollow CoPt materials are much greater than those of Pt and CoPt nanoparticles, indicating larger ECSA for hollow Co-Pt spheres due to their hollow spherical structure. They also claimed that, $Co_{32}Pt_{68}$ spheres exhibited better activity at 0.5 V in comparison to those of other nanoparticles of Pt and CoPt. The transformation in the lattice structure or the electronic properties of the Co-Pt bimetal at this potential is responsible for the greater electrochemical performance. Zhou et al. also mentioned the synthesis of PtNi hollow nanospheres, which were applied as electrocatalysts in methanol oxidation reaction [120]. They compared their results with commercial Pt/C electrocatalyst (Johnson-Matthey, 20 wt% Pt). The cyclic voltammetric results confirmed the better electrocatalytic performance of PtNi Hollow nanospheres, in comparison to the commercial one. It is known that the ratio of anodic peak current in forward (I_f) and (I_b) is the key factor in the tolerance of a catalyst to intermediates generated during the methanol oxidation [126]; a low I_f/I_b value indicates the poor methanol electrooxidation to CO during the forward scan of the CV; therefore, excessive amount of carbonaceous intermediates will be accumulated on the catalyst surface [127]. In this study, this value is 1.14 times for PtNi hollow sphere as that of commercial catalyst. Thus, hollow sphere catalysts have shown better poison tolerance. Hu et al. also reported the electrocatalytic activity of mesoporous PtNi nano-hollow spheres (HMPNNs) in methanol electrooxidation [119]. According to their results, the HMPNNs also showed better poison tolerance activity than that of solid PtNi nanospheres and commercially available Pt. The electrochemical activities were measured in 0.5 M H_2SO_4 solution as electrolyte. They estimated electrochemical surface areas (ECSAs) for HMPNNs as 88.5 m^2/g_{Pt}, which were 1.5 and 1.7 times than those of solid PtNi nanospheres and commercial Pt catalysts. The onset potential value is much lower (260 mV negative shift compared to solid PtNi nanospheres) for HMPNNs. They explained the enhanced electrocatalytic activity of hollow nanospheres of PtNi, due to the unique hollow mesoporous structures together with the synergistic role of Pt and Ni in the catalysts. It is known that Ni alloying actually reduces the electronic binding energy in Pt and facilitates the C-H cleavage reaction in methanol decomposition [127]. At the same time, the pores situated in shells enhanced the activity by increasing the surface areas and inducing the atomic surface structures. Therefore, the interior surface of the spheres becomes available for the guest species from the outside, resulting in the great electrocatalytic performance for the nano-hollow spherical PtNi compounds.

Guo et al presented PtRu nano-hollow spheres on multiwalled carbon nanotubes (MWCNTs), which were utilized as electrocatalysts in methanol electrooxidation reaction [96]. It is already established that Pt and Pt-based electrocatalyst particles should be supported on carbon surfaces. The supported nanoparticles exhibit better electrocatalytic activity and utilization efficiency than those of unsupported metal particles for their large surface area on the supports [121,128]. Guo et al. considered CNTs as new supports for their metal, due to their small size, high chemical stability and large surface area to volume ratio [96]. The electrochemical measurements of hollow nano PtRu/MWCNTs (HN-PtRu/MWCNTs), solid nano PtRu/MWCNTs (SN-PtRu/MWCNTs) and E-TEK Pt/C nanoparticles were performed in a 1.0 M $HClO_4$ aqueous solution containing 1.0 M methanol. The cyclic voltammograms showed electrocatalytic activity of all the materials, although HN-PtRu/MWCNTs exhibited the best. The remarkably high oxidation current is directly related to the high surface area value for hollow sphere electrocatalysts. Since PtRu hollow nanospheres are coreless in structure, a larger number of PtRu nanospheres are formed with the same loading of PtRu nanoparticles. The inner surface of PtRu hollow structures should have much higher activity than the outer surface, as the curvature radii of the inner surface are smaller than that of the outer surface. On the other hand, the potential value for the methanol oxidation reaction is much lower for HN-PtRu/MWCNTs and SN-PtRu/MWCNTs compared to that of commercial PtRu/C electrocatalysts. The chronoamperometry results also showed higher values of initial and limiting currents for hollow PtRu materials, indicating the larger electrocatalytic activity in methanol electrooxidation reaction, relative to the other materials. They also performed CO stripping voltammetry to determine the CO electro-oxidizing ability of the materials, as CO species are the main poisoning intermediate. The results indicated the onset potential of CO oxidation at 0.26 V, which is much lower than that of other electrocatalysts under consideration in their work. In all the experiments, Pt gauze and a saturated calomel electrode (SCE) were used as counter electrode and reference electrode, respectively. It confirms the beneficial role of the hollow nanospheres of PtRu materials. The same research group later reported a similar approach with PtCo nano-hollow sphere over multiwalled carbon nanotubes [95]. According to the cyclic voltammetry and chronoamperometric studies, HN-PtCo/MWCNTs had better electrocatalytic performance in comparison to that of SN-PtCo/MWCNTs and Pt/C materials. The authors explained that the incomplete and porous shells of the PtCo hollow nanospheres with higher surface area and ideal surface structure influenced the enhanced electrocatalytic performance in methanol oxidation. Similarly, the diameter of the semicircle formed in Nyquist plots is considerably small for HN-PtCo/MWCNTs, which confirms the facile methanol oxidation in presence of hollow spherical bimetallic. Similar work also reported by Guo et al. with Au-Pt core-shell nanomaterials with hollow cavity with their electrocatalytic approach in methanol electro-oxidation and oxygen reduction reaction [129], although in this section only methanol electro-oxidation activity will be

mentioned. The cyclic voltammetries were performed using Au-Pt hollow nanospheres in comparison with hollow gold nanospheres, modified gold electrode and Pt electrode in 0.5 M H_2SO_4 solution containing 1 M methanol with the scan rate of 50 mV sec^{-1}. The peak current in the forward direction is much improved with Au-Pt materials, due to their sponge-like characteristics. The I_f/I_b ratio of sponge-like hybrid hollow nanosphere is 2.57, which is higher than that of the E-TEK catalyst (0.74).

Nickel hollow spheres were also reported as electrocatalysts in methanol and ethanol electrooxidation reaction by Xu et al. [99]. The high price and limited supply of Pt electrocatalysts in direct alcohol fuel cells shifted the attraction towards economically favorable Ni hollow spherical materials. They presented cyclic voltammograms of methanol and ethanol electrooxidation reaction in 1.0 M KOH containing 1.0 M alcohol with the potential range of −0.8 V to 0.3 V. A platinum foil (3.0 cm^2) and Hg/HgO (1.0 M KOH) were used as counter and reference electrode, respectively. They explained the initial oxidation of nickel to $Ni(OH)_2$ formation, which was gradually converted to NiOOH compound, created small lumps in the anodic sweep of the voltammograms [130]. During the reaction, alcohol was further oxidized and $Ni(OH)_2$ was converted back. Xu et al. clearly emphasized the reaction scheme during the alcohol oxidation. The peak current density values mentioned by them with Ni hollow spheres were 25 and 17 mA cm^{-2} for methanol and ethanol oxidation, which was far better electrocatalytic activity in comparison with the Ni particles. In the same context, the onset potential value for nickel hollow spheres was 350 mV negative with respect to those of Ni particles in methanol and ethanol electrooxidation. In an electrochemical reaction, electrode surfaces are highly sensitive to any redox active species, which are able to diffuse to the electrode/electrolyte interface during an electrochemical reaction [131]. In this case, the hollow structure of spherical materials makes larger three-phase interface, and liquid alcohol will easily be diffused into the catalysts layers, resulting in the reduction of liquid sealing effect and concentration polarization. These materials induce liquid fuel to diffuse inside and products will be diffused out of the catalyst layer. In this way, the utilization efficiency of nickel hollow sphere catalysts has been explained [95]. Similarly, Dai et al. mentioned the electrocatalytic activity of Pd hollow spheres direct electro-oxidation of ethanol [114]. Cyclic voltammogram and chronoamperometric studies were performed with and without ethanol in 1 M KOH solution. The onset potential was 43 mV negative in comparison to that of Pd film electrode. The peak current density value was remarkably higher (222 mA cm^{-2}) with Pd hollow sphere array. The higher I_f/I_b value indicates that the Pd hollow sphere array has excellent anti-poison capability.

All the metal hollow spherical materials presented higher electrocatalytic performance in methanol electro-oxidation reaction in comparison with their non-hollow spherical counterpart. They always get beneficial due to their porous outer structure with void space inside the spheres, which makes them advantageous in electrocatalytic activity.

2. Metal Sphere Electrocatalysts in Water Electrolysis

Water electrolysis represents the most important process to produce hydrogen without evolution of CO_2. Moreover, the process offers a way to convert electrical energy to chemical energy as hydrogen and oxygen production, which can further be converted back to electrical energy when needed.

$$2H_2O \rightarrow O_2 + 4H^+ + 4e^-$$

At the same time, O_2 evolution is the most common anodic reaction coupled with most of the cathodic processes occurring in aqueous solutions (water electrolysis and metal electrowinning), which is an unavoidable side reaction in many anodic processes [132]. Normally, the oxygen evolution electrode is the component of the system which has the largest over-potential at typical operating current densities.The major problems in hydrogen and oxygen production from water electrolysis are high energy consumption, mainly due to the high production and investment cost. In recent days, researchers are considered the following things during preparation of electrocatalysts: the minimization of the platinum metal loading; alloying of platinum with transition metals to improve catalytic activity (Pt-Co, Pt-Ni, Pt-Fe, Pt-Ru, Pt-Pd, Pt-Rh and Pt-Sn catalysts) [133,134]; use of comparatively stable mixed oxides to increase the long term stability of electrode, to improve product selectivity and/or to minimize overpotentials. Now-a-days, electrodes based on dispersed precious metal on an inert high area substrate (most commonly, formulated from carbon powder) are among the workhorses of electrochemical technology [135]; as on the longer timescale of pilot plant operation, precious metals like platinum are often found to corrode significantly [136]. The hydrogen evolution reaction (HER) is the main reaction in water electrolysis and has been one of the most studied electrochemical reactions [137]. It is well-known that HER occurs via two successive steps:: (a) the initial discharge of hydronium ion (H_3O^+) to form adsorbed hydrogen atom $H_{(a)}$ (Volmer step) is presented below:

$$H_3O^+ + 1e^- \rightarrow H_{(a)} + H_2O$$

This step will be followed by the Tafel step in which two adsorbed H atoms recombine to form H_2 molecule.

$$2H_{(a)} \rightarrow H_2$$

Otherwise, the first step can be followed by a reaction in which adsorbed H with H_3O^+ in the solution (Heyrovsky step) producing H_2.

$$H_{(a)} + H_3O^+ \rightarrow H_2 + H_2O$$

HER is generally believed to occur via Volmer-Tafel mechanism with the later step being the rate determining one [138]. Tafel slopes ca. 30 mV dec^{-1} were reported for Pt metal crystalline (111) (110) and (100) phases in acidic media [139-141]. The alloyed compounds with low Pt content are popular as electrode materials in fuel cells [142,143]. These electrocatalysts are significantly influenced by the dispersion, size, and shape of the crystalline metal in the electrode material. Therefore, the sub-micrometer and nanometer-sized hollow spheres with tunable shell thickness, large surface area and void volume are implied as successful electrocatalysts in water electrolysis. Metal doped titania hollow spheres have shown effective electrocatalytic activity in aqueous and PEM water electrolysis both in hydrogen and oxygen evolution reactions [81, 82]. Initially, Kim et al. reported Pt-doped titania hollow spheres

in aqueous water electrolyzer in acidic media [81]. The CV curves presented that 20 wt% Pt-doped TiO_2 (calcined at 400 °C) has remarkably high anodic peak current density of 11 mA cm^{-2} at 1.9 V in comparison with the others, which resulted in the evolution of oxygen gas during anodic sweep. Similarly, one small peak also appeared around 1.6 V in the cathodic sweep of voltammogram in each of the CV curves of 20 wt% Pt-doped titania catalysts calcined at various temperatures; this peak indicates the reduction of oxygen. The hollow spherical structures with high surface area value (125-215.2 m^2 g^{-1}) induced the electrochemical activity of these materials. Savych et al. worked on Nb-doped TiO_2 fibres, which were further doped with Pt nano-particles [144]. They showed quite low current density value in linear sweep voltammetry in comparison to the Pt-doped on TiO_2 hollow spherical structures [81]. At the same time, they came up with very poor surface area value of 15-87 m^2 g^{-1}. Gebauer et al. also worked on Pt nanoparticles doped on TiO_2 electrocatalysts in ORR for PEM fuel cell [133]. For these materials the kinetic current densities were highest on the Pt/TiO_2 catalyst, which might have been related to metal-support interactions.

Among the oxygen evolution electrocatalysts, IrO_x has been extensively investigated, which has proven to have 20 times longer service life than RuO_2 [145]. Otherwise, IrO_x is much more expensive than RuO_2, and its activity is slightly lower [146]. An extensive search therefore has been carried out in the laboratory for addition of suitable combination of O_2 evolution electrocatalysts to save the cost and/or to improve the coating property. It was found that IrO_x-Ta_2O_5 was the best pair among various combinations. Other O_2 evolution electrocatalysts of interest include IrO_x-TiO_2-CeO_2 [147] and SnO_2-$CuCo_2O_4$ [148]. In the literature, SnO_2 has been used mostly in O_2 evolution electrocatalysts to increase the electrochemical stability of the catalyst and as a dispersing material. But actually SnO_2 is a semiconductor by itself, which can enhance the conductivity at the surface of the catalyst to a great extent. In Sn-doped TiO_2 hollow sphere electrocatalysts, similar physicochemical property between SnO_2 and TiO_2 with wide band gaps (TiO_2~3.05 eV; SnO_2~3.5 eV) [146] influenced their great electrocatalytic property [82]. In cyclic voltammetric study, present in Fig. 11, two distinguished anodic peaks had appeared, considered as the hydrogen desorption from the bulk of the metal together with desorption of hydrogen adsorbed on the metal surface [133,149-151]. Similarly, other two counterparts were ascribed as the molecular hydrogen evolution during cathodic sweep. These four peaks were interpreted as weakly and strongly bonded hydrogen adatoms on the catalyst surface [133]. Besides, one single peak was also observed most prominently at 1.21 V in 20 wt% Sn/TiO_2, which faded away consecutively with increase in the tin loading. This small peak is attributed to the oxygen reduction reaction (ORR). Electrochemical ORR with 4-electron pathway is highly preferred in acidic aqueous solution around 1.2 V of thermodynamic potential value.

$$O_2+4\,H^++e^-\rightarrow H_2O$$

The anodic peak current density value (O_2 evolution) was observed around 7 mA cm^{-2} for all the tin-doped hollow spheres; whereas hydrogen evolution was intense in 20 and 40 wt% Sn doped TiO_2 samples calcined at 300 °C. It can also be concluded that electrocatalytic activity for HER was influenced considerably with increase in calcinations temperature. Anodic polarization curve for Sn-doped titania hollow spheres confirms the inclining trend in electrocatalytic activity with rise in the calcinations temperature (Fig. 12) [82].

Ba and Ni doped titania hollow sphere electrocatalysts had a similar trend in cyclic voltammograms, although their activity proved better both in HER and OER in comparison with Tin loaded materials [82-84]. On the basis of XRD and TEM results of Ba/TiO_2 hollow sphere materials, it is clear that the surface of the hollow sphere catalysts is covered with $BaTiO_3$ and TiO_2 phases; thus, both the phases contributed in the electrocatalytic properties of Ba-doped TiO_2 hollow sphere materials. The results also implied that the sample with prominent rutile TiO_2 phase (20 wt% Ba/TiO_2) exhibited best activity in oxygen evolution and reduction during electrolysis (Fig. 13) [83]. Although the samples treated with greater

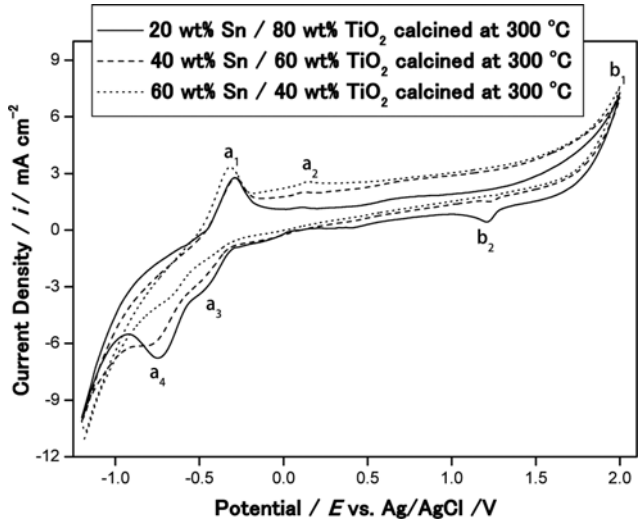

Fig. 11. Cyclic voltammograms of Sn-doped TiO_2 hollow spheres in aqueous cell [82].

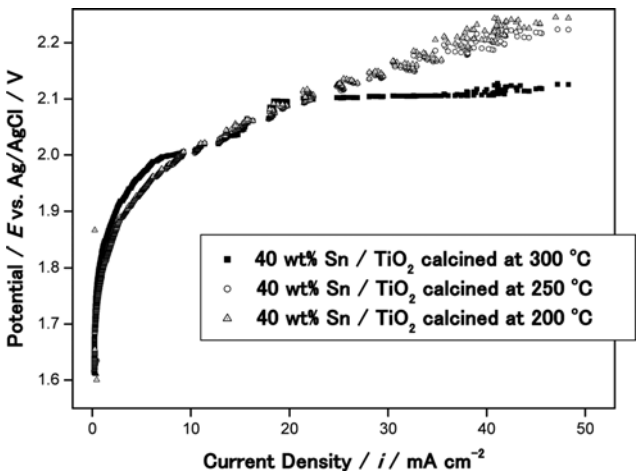

Fig. 12. Anodic polarization curves of 40 wt% Sn-doped TiO_2 hollow spheres calcined at 200, 250, and 300 °C [82].

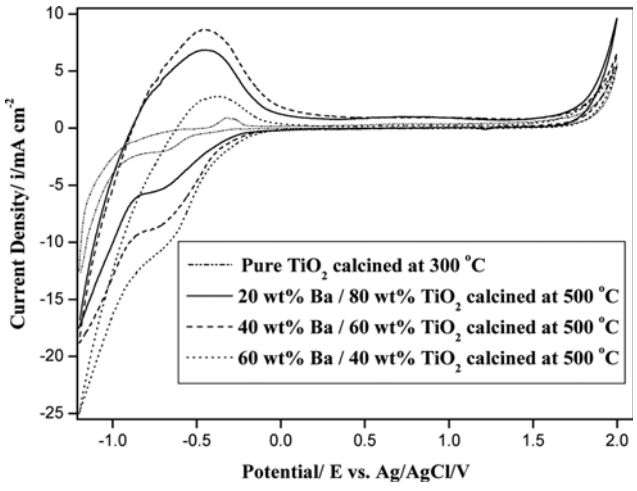

Fig. 13. Cyclic voltammograms of Ba-doped TiO_2 hollow spheres in aqueous cell [83].

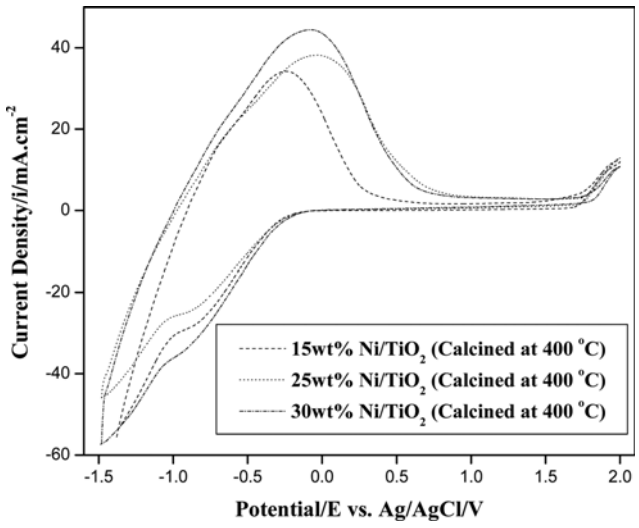

Fig. 14. Cyclic voltammograms of Ni/TiO_2 hollow spheres in aqueous cell [84].

calcination temperature had created more prominent growth of $BaTiO_3$ and rutile TiO_2 phase, the anodic and cathodic peak current density value was reduced greatly for the catalyst with 700 °C calcination temperature, which was ascribed to its reduced surface area value. In the literature, barium titanate ($BaTiO_3$) is considered as one of the most important ferroelectric oxides used in electronic purposes. Among various defects, oxygen vacancies are thought to be the most mobile and abundant in this perovskite ferroelectric. These oxygen vacancies play an important role in adsorption of oxygen during the electrolysis process. On the other hand, the well-known oxygen deficient nature of titania also enhances the oxygen adsorption and diffusion process through the oxygen vacancies present on the catalyst surface. Among the barium-doped hollow spheres, 20 wt% Ba-doped material (calcined at 500 °C) had acted best in oxygen evolution reaction with anodic current density value of 60 mA cm^{-2} at comparatively lower over-potential value during anodic polarization measurements; whereas, tin-doped hollow sphere materials only produced 50 mA cm^{-2} of anodic current density at similar over-potential value [82]. On the other hand, Ni/TiO_2 hollow sphere electrocatalysts have been evaluated up to 53 mA cm^{-2} in anodic polarization experiments. During cyclic voltammetric tests, anodic peak current density value, which usually represents the oxygen evolution phenomenon, was revealed as 13 mA cm^{-2} for 25 wt% Ni-loaded sample, whereas the hydrogen evolution peak was most intense for 30 wt% Ni/TiO_2 material with cathodic peak current density of 32 mA cm^{-2} [84].

The physical and electrochemical characterization results of Ni-doped hollow sphere materials revealed that the catalysts with more intense NiO phase and less intense rutile TiO_2 phase have worked in hydrogen desorption reaction present in anodic sweep; whereas oxygen evolution peaks are more intense with samples with more intense rutile TiO_2 phase. Thus, it can be concluded that the presence of both NiO and TiO_2 phases has contributed in the electrocatalytic activity of hollow sphere samples. Oxygen deficient nature of titania could have created oxygen vacancies on the catalyst surface, especially on the (110) phase of TiO_2 [152]. On the other hand, nickel monoxide, NiO, exhibits a cubic NaCl structure with a lattice parameter of 0.4173 nm [153,154]. The NiO always exhibits an excess of oxygen, although the extra oxygen cannot be placed inside the NaCl structure; instead vacancies related to Ni^{2+} are created, thus giving a p-type conduction character [155]. It is known that excess oxygen in NiO produces a Ni^{2+} vacancy, which leads to the creation of a hole on two adjacent Ni^{2+} ions, resulting in the yield of Ni^{3+} ions. Similarly, both the oxides exhibit strong hydrogen adsorption property. Therefore, both oxygen and hydrogen are adsorbed on the hollow sphere surface and also into the void sphere of the samples. From the SEM and TEM images, it is clear that both the gases could enter into the sphere through the pores present all over the sphere. The oxygen adsorption phenomenon at vacancies results in the charge shifting and alteration of the local electronic structure on the semiconductor surface. Fig. 14 represents the cyclic voltammograms for Ni-doped titania hollow sphere electrocatalysts [84]. In the cathodic sweep, oxygen is partially reduced through the interaction of oxygen molecule with Ti^{3+} and Ni^{+} ions, which usually generates at large cathodic potential range. On the catalyst surface, Ti^{4+} and Ni^{2+} matrix are acting as electron excess sites. Thus, oxygen molecules always try to compete for more reduced metal ions, resulting in the unsymmetrical reduction process, with only one oxygen atom bonded to the surface. This oxygen reduction process therefore resulted in the hydrogen evolution during the electrolysis process. The same electrocatalysts had also been reported for application in polymer electrolyte membrane (PEM) electrolyzer. The performance of the PEMWE system mainly depends on the structure and electrochemical characteristics of the electrode materials involved in hydrogen and oxygen evolution reaction. The efficiency of MEA is entirely dependent on the material characteristics of both the electrodes and membranes as well as on the structure of triple-phase boundary [156,157]. According to cyclic voltammograms present in Fig. 15, 30 wt% Ni-loaded titania hollow spheres were established as the best electrocatalysts in HER with 0.36 A cm^{-2} peak current density value [85]. On the contrary, 15 wt% Ni/TiO_2 hollow sphere sample is most active in OER with anodic peak cur-

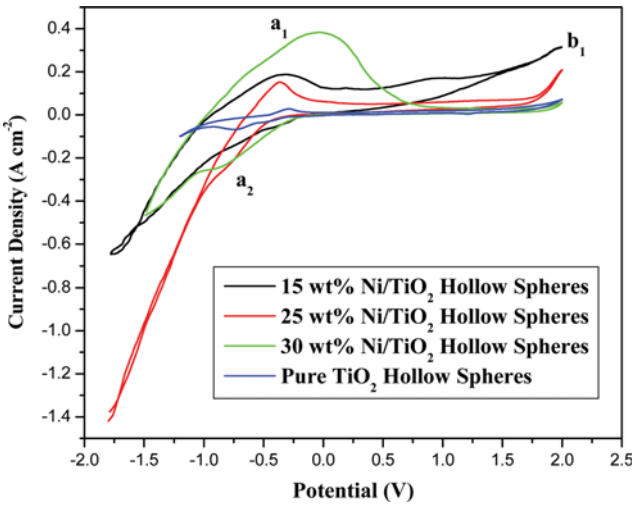

Fig. 15. Cyclic voltammograms of Ni/TiO_2 hollow spheres in PEM water electrolysis cell [85].

rent density of 0.3 A cm^{-2}. Both the values are quite higher than those of their corresponding activities in aqueous cell. The polarization curves also confirmed that 30 wt% Ni-doped TiO_2 hollow sphere electrocatalyst has acquired superior catalytic activity in HER compared with others. On the other hand, the performance of 15 wt% Ni/TiO_2 hollow sphere electrocatalyst was evaluated up to 140 mA cm^{-2} at comparatively lower over-potential value.

All these metal doped hollow sphere materials have been reported as stable electrocatalysts in acidic media for 48-72 h at potentiostatic conditions [81-84]. In all the cases, the hollow sphere structure of the catalysts enhanced the adhesion quality towards carbon cloth (on which catalyst ink was loaded). Thus, the catalysts ink was stuck with the substrate for long time and showed stable electrochemical activity.

CONCLUSIONS

Over the past few decades, considerable improvement has been noticed in the synthesis and application of inorganic hollow structures. The present review article emphasizes especially the electrochemical application of hollow spherical structures, including their synthetic approach. Hard and sacrificial templating methods are arguably the most effective synthesis methods in hollow spherical electrocatalysts. Several drawbacks can be mentioned in hard templating method, which range from the inherent difficulty of achieving high product yields from the multistep synthetic process to the lack of structural robustness of the shells during removal of core template. In sacrificial templating synthetic approach, these complications regarding template removal can conveniently be overcome. The literature survey shows that high-quality hollow particles with non-agglomerated, uniform and controlled size, are remarkably advantageous in electrochemical applications, but the synthetic approach towards this application is still limited. Moreover, these synthesis methods of both templating and without templating technologies include very low precursor concentration, resulting in a challenging situation when they scale-up to commercial scale quantities. Although these hollow structures are widely popular in every industrial field, still the approach in electrochemical industries is rare. Metal hollow structures are mainly popular in methanol electrooxidation (for methanol fuel cell) and HER & OER (for water electrolyzer) process. The high surface area with void inner space can offer exciting opportunities in every aspect of electrochemical technology. Among metal-doped titania hollow sphere electrocatalysts, Ni materials have worked best in the HER process. The electrocatalytic activity has also been enhanced with greater loading of doped metals. In methanol electro-oxidation reaction, PtRu hollow spheres performed well in comparison to their other counterparts. Thus, these inorganic hollow structured materials can initiate a new era in this field, if synthetic strategies are approached as per requirement. At the same time, spherical structure with multi-shell and greater pore size can be a potential candidate in the electrochemical industry, provided the synthetic approach could be simpler.

REFERENCES

1. Y. Xia and R. Mokaya, *J. Mater. Chem.*, **153**, 126 (2010).
2. S. H. Xuan, W. Q. Jiang, X. L. Gong, Y. Hu and Z. Y. Chen, *J. Phys. Chem. C*, **113**, 553 (2009).
3. J. Chattopadhyay, R. Srivastava and P. K. Srivastava, *Int. J. Electrochem. Sci.*, **8**, 3740 (2013).
4. W. Wu, X. Xiao, S. Zhang, F. Ren and C. Jiang, *Nanoscale Res. Lett.*, **6**, 533 (2011).
5. J. Livage, *Materials*, **3**, 4175 (2010).
6. J. G. Wang, F. Li, H. J. Zhou, P. C. Sun, D. T. Ding and T. H. Chen, *Chem. Mater.*, **21**, 612 (2009).
7. R. Rengarajan, P. Jiang, V. Colvin and D. Mittleman, *Appl. Phys. Lett.*, **77**, 3517 (2000).
8. X. Lai, J. Li, B. A. Korgel, Z. Dong, Z. Li, F. Su, J. Du and D. Wang, *Angew. Chem.*, **50**, 2738 (2011).
9. X. Liu, J. Zhang, X. Guo, S. Wu and S. Wang, *Sens. Actu. B: Chem.*, **152**, 162 (2011).
10. H. S. Hou, X. Cao, Y. Yang, L. Fang, C. Pan, X. Yang, W. Song and X. Ji, *Chem. Commun.*, **50**, 8201 (2014).
11. G. Yang, S. Gai, F. Qu and F. P. Yang, *Appl. Mater. Inter.*, **5**, 5788 (2013).
12. F. Cheng, H. Ma, Y. Li and J. Chen, *Inorg. Chem.*, **46**, 788 (2007).
13. L. Xie, J. Zheng, Y. Liu, Y. Li and X. Li, *Chem. Mater.*, **20**, 282 (2008).
14. J. Chattopadhyay, R. Srivastava and P. K. Srivastava, *J. Appl. Electrochem.*, **43**, 279 (2013).
15. J. E. Son, J. Chattopadhyay and D. Pak, *Int. J. Hydrogen Energy*, **35**, 420 (2010).
16. H. Ren, R. Yu, J. Wang, Q. Jin, M. Yang, D. Mao, D. Kisailus, H. Zhao and D. Wang, *Nanolett.*, **14**, 6679 (2014).
17. S. Xu, C. M. Hessel, H. Ren, R. Yu, Q. Jin, M. Yang, H. Zhao and D. Wang, *Energy Environ. Sci.*, **7**, 632 (2014).
18. J. Wang, N. Yang, H. Tang, Z. Dong, Q. Jin, M. Yang, D. Kisailus, H. Zhao, Z. Tang and D. Wang, *Angew. Chem.*, **52**, 6417 (2013).
19. J. Qi, K. Zhao, G. Li, Y. Gao, H. Zhao, R. Yu and Z. Tang, *Nanoscale*, **6**, 4072 (2014).
20. J. Du, J. Qi, D. Wang and Z. Tang, *Energy Environ. Sci.*, **5**, 6914

(2012).
21. Z. Dong, H. Ren, C. M. Hessel, J. Wang, R. Yu, Q. Jin, M. Yang, Z. Hu, Y. Chen, Z. Tang, H. Zhao and D. Wang, *Adv. Mater.*, **26**, 905 (2014).
22. W. Jiao, X. Hu, H. Ren, P. Xu, R. Yu, J. Chen and X. Xing, *J. Mat. Chem. A*, **2**, 18171 (2014).
23. P. Xu, R. Yu, H. Ren, L. Zong, J. Chen and X. Xing, *Chem. Sci.*, **5**, 4221 (2014).
24. C. Xu, L. Wang, R. Wang, K. Wang, Y. Zhang, F. Tian and Y. Ding, *Adv. Mater.*, **21**, 2165 (2009).
25. P. Gómez-Romero and C. Sanchez, Hybrid materials, functional applications. An introduction. In Functional Hybrid Materials; P. Gómez-Romero, C. Sanchez, Eds. Wiley-VCH Verlag GmbH & Co. KGaA: Weinheim, Germany, pp. 1-14 (2004).
26. A. Fahmi, T. Pietsch and C. Mendoza, *Mater. Today*, **12**, 44 (2009).
27. G. L. Athens, R. M. Shayib and B. F. Chmelka, *Curr. Opinion Col. Inter. Sci.*, **14**, 281 (2009).
28. V. Fischer, I. Lieberwirth, G. Jakob, K. Landfester and R. M. Espí, *Adv. Func. Mater.*, **23**, 451 (2013).
29. S. Neyshtadt, J. P. Jahnke, R. J. Messinger, A. Rawal, S. Peretz, D. Huppert, B. F. Chmelka and G. L. Frey, *J. Am. Chem. Soc.*, **133**, 10119 (2011).
30. Z. Yang, Z. Niu, Y. Lu, Z. Hu and C. C. Han, *Angew. Chem.*, **115**, 1987 (2013).
31. R. A. Caruso, A. Susha and F. Caruso, *Chem. Mater.*, **13**, 400 (2001).
32. H. Xu and W. Wang, *Angew. Chem.*, **46**, 1489 (2007).
33. J. Hu, M. Chen, X. Fang and L. Wu, *Chem. Soc. Rev.*, **40**, 5472 (2011).
34. N. A. Dhas and K. S. Suslick, *J. Am. Chem. Soc.*, **127**, 2368 (2005).
35. J. J. Zhu, S. Xu, H. Wang, J. M. Zhu and H. Y. Chen, *Adv. Mater.*, **15**, 156 (2003).
36. M. Titrici, M. Antonietti and A. Thomas, *Chem. Mater.*, **18**, 3808 (2006).
37. J. Yu and X. Yu, *Env. Sci. Technol.*, **42**, 4902 (2008).
38. M. Xu, L. Kong, W. Zhou and H. Li, *J. Phys. Chem. C*, **111**, 19141 (2007).
39. J. Yang, J. Y. Lee, H.-P. Too and S. Valiyaveettil, *J. Phys. Chem. B*, **110**, 125 (2006).
40. S. Guo, S. Dong and E. Wang, *Chem. Eur. J.*, **14**, 4689 (2008).
41. H. M. Chen, R. S. Liu, M. Y. Lo, S. C. Chang, L. D. Tsai, Y. M. Peng and J. F. Lee, *J. Phys. Chem. C*, **112**, 7522 (2008).
42. H. Liu, J. Qu, Y. Chen, J. Li, F. Ye, J. Y. Lee and J. Yang, *J. Am. Chem. Soc.*, **134**, 11602 (2012).
43. H. Liu, F. Ye and J. Yang, *Ind. Eng. Chem. Res.*, **53**, 5925 (2014).
44. F. Caruso, R. A. Caruso and H. Möhwald, *Science*, **282**, 1111 (1998).
45. F. Caruso, X. Shi, R. A. Caruso and A. Susha, *Adv. Mater.*, **13**, 740 (2001).
46. I. Tissot, C. Novat, F. Lefebvre and E. Bourgeat-Lami, *Macromolecules*, **34**, 5734 (2001).
47. P. Jiang, J. F. Bertone and V. L. Colvin, *Science*, **291**, 453 (2001).
48. H. Shiho and N. Kawahashi, *Colloid. Polym. Sci.*, **278**, 270 (2000).
49. S. Eiden and G. Maret, *J. Colloid Interface Sci.*, **250**, 281 (2002).
50. Z. Zhong, Y. Yin, B. Gates and Y. Xia, *Adv. Mater.*, **12**, 206 (2000).
51. W. Li, X. Sha, W. Dong and Z. Wang, *Chem. Commun.*, **20**, 2434 (2002).
52. D. Zhang, L. Qi, J. Ma and H. Cheng, *Adv. Mater.*, **14**, 1499 (2002).
53. K. J. C. van Bommel, J. H. Jung and S. Shinkai, *Adv. Mater.*, **13**, 1472 (2001).
54. M. H. Wu and G. M. Whitesides, *Adv. Mater.*, **14**, 1502 (2002).
55. S. L. Che, K. Takada, K. K. Takashima, O. Sakurai, K. Shinozaki and N. Mizutani, *J. Mater. Sci.*, **34**, 1313 (1999).
56. Y. Syuama and A. Kato, *Ceram. Int.*, **8**, 17 (1982).
57. J. H. Bang, R. J. Helmich and K. S. Suslick, *Adv. Mater.*, **20**, 2599 (2008).
58. L. Mädler and S. E. Pratsinis, *J. Am. Cer. Soc.*, **85**, 1713 (2002).
59. L. Wang and Y. Yamauchi, *J. Am. Chem. Soc.*, **135**, 16762 (2013).
60. Y. F. Lu, H. Fan, A. Stump, T. L. Ward, T. Rieker and C. J. Brinker, *Nature*, **398**, 223 (1999).
61. G. Q. Jian, L. Liu and M. R. Zachariah, *Adv. Func. Mater.*, **23**, 1341 (2013).
62. X. W. Lou, L. A. Archer and Z. Yang, *Adv. Mater.*, **20**, 3987 (2008).
63. J. Qi, X. Lai, J. Wang, H. Tang, H. Ren, Y. Yang, Q. Jin, L. Zhang, R. Yu, G. Ma, Z. Su, H. Zhao and D. Wang, *Chem. Soc. Rev.*, **44**, 6749 (2015).
64. G. K. Chandler, J. D. Genders and D. Pletcher, *Platinum Met. Rev.*, **41**, 54 (1997).
65. B. Simon, S. Ziemann and M. Weil, Metal Res Tech DOI:http://dx.doi.org/10.1051/metal/2014010.
66. H. G. Ayagh, S. Jolly, D. Patel, J. Hunt, W. A. Steen, C. F. Richardson and O. A. Marina, *ECS Trans.*, **51**, 265 (2013).
67. J. Maier, *Nat. Mater.*, **4**, 805 (2005).
68. H. Liang, H. Zhang, J. Hu, Y. Guo, L. Wan and C. Bai, *Angew. Chem.*, **43**, 1540 (2004).
69. J. Wu, Z. Peng and H. Yang, *Phy. Trans. R Soc. A*, **368**, 4261 (2010).
70. J. Wang, H. Tang, H. Ren, R. Yu, J. Qi, D. Mao, H. Zhao and D. Wang, *Adv. Sci.* 1 (2014), DOI:10.1002/advs.201400011.
71. W. Zhao, M. Lang, Y. Li, L. Li and J. Shi, *J. Mater. Chem.*, **19**, 2778 (2009).
72. X. S. Zhao, F. Su, Q. Yan, W. Guo, X. Y. Bao, L. Lv and Z. Zhou, *J. Mater. Chem.*, **16**, 637 (2006).
73. H. Li, Z. Bian, J. Zhu, D. Zhang, G. Li, Y. Huo, H. Li and Y. Lu, *J. Am. Chem. Soc.*, **129**, 8406 (2007).
74. X. Lai X, J. E. Halpart and D. Wang, *Energy Environ. Sci.*, **5**, 5604 (2012).
75. Y. Zeng, X. Wang, H. Wang, Y. Dong, Y. Ma and J. Yao, *Chem. Comm.*, **46**, 4312 (2010).
76. T. Peng, A. Hasegawa, J. Qiu and K. Hirao, *Chem. Mater.*, **15**, 2011 (2003).
60. L. Z. Wang, S. Tomura, M. Maeda, F. Ohashi, K. Inukai and M. Suzuki, *Chem. Lett.*, **12**, 1414 (2000).
77. D. H. Chen, F. Z. Huang, Y. B. Cheng and R. A. Caruso, *Adv. Mater.*, **21**, 2206 (2009).
78. A. Imhoff, *Langmuir*, **17**, 3579 (2001).
79. M. Li, H. Tan, L. Chen, J. Wang and S. Y. Chou, *J. Vac. Sci. Tech. B*, **21**, 660 (2003).
80. D. Wang, C. Song, Y. Lin and Z. Hu, *Mater. Lett.*, **60**, 77 (2006).
81. H. R. Kim, J. Chattopadhyay, J. I. Son and D. Pak, *Korean J. Chem. Eng.*, **25**, 775 (2008).
82. J. Chattopadhyay, H. R. Kim, S. B. Moon and D. Pak, *Int. J. Hydrogen Energy*, **33**, 3270 (2008).
83. J. E. Son, J. Chattopadhyay and D. Pak, *Int. J. Hydrogen Energy*, **35**, 420 (2010).

84. J. Chattopadhyay, R. Srivastava and P. K. Srivastava, *J. Appl. Electrochem.*, **43**, 279 (2013).
85. J. Chattopadhyay, R. Srivastava and P. K. Srivastava, *Korean J. Chem. Eng.*, **30**, 1571 (2013).
86. J. Hu, M. Chen, X. Fang and L. Wu, *Chem. Soc. Rev.*, **40**, 5472 (2011).
87. M. Sashidharan, K. Nakashima, N. Gunwardhana, T. Yokoi, M. Inoue, S. Yusa, M. Yoshio and T. Tatsumi, *Chem. Comm.*, **47**, 6921 (2011).
88. A. Imhof and D. J. Pine, *Nature*, **389**, 948 (1997).
89. A. Imhof and D. J. Pine, *Adv. Mater.*, **10**, 697 (1998).
90. H. Zhang, G. C. Hardy, Y. Z. Khimyak, M. J. Rosseinsky and A. I. Cooper, *Chem. Mater.*, **16**, 4245 (2004).
91. T. Nakashima and N. Kimizuka, *J. Am. Chem. Soc.*, **125**, 6386 (2003).
92. S. Guo, Y. Fang, S. Dong and E. Wang, *J. Phys. Chem. C*, **111**, 17104 (2007).
93. M. Chen and L. Gao, *Inorg. Chem.*, **45**, 5145 (2006).
94. J. Qu, H. Liu, F. Ye, W. Hu and J. Yang, *Int. J. Hydrogen Energy*, **37**, 13191 (2012).
95. D. J. Guo and S. K. Cui, *J. Col. Inter Sci.*, **340**, 53 (2009).
96. D. J. Guo, L. Zhao, X. P. Qiu, L. Q. Chen and W. T. Zhu, *J. Power Sources*, **177**, 334 (2008).
97. J. Wei, X. Wang, Y. Wang, Q. Chen, F. Pei and Y. Wang, *Int. J. Hydrogen Energy*, **34**, 3360 (2009).
98. A. Henglein and M. Giersig, *J. Phys. Chem. B*, **103**, 9533 (1999).
99. C. Xu, Y. Hu, J. Rong, S. P. Jiang and Y. Liu, *Electrochem. Commun.*, **9**, 2009 (2007).
100. S. L. Westcott, S. J. Oldenberg, T. R. Lee and N. J. Halas, *Langmuir*, **14**, 5396 (1998).
101. Z. J. Jiang and C. Liu, *J. Phys. Chem. B*, **107**, 12411 (2003).
102. A. D. Smigelskas and E. O. Kirkendall, *Trans. Am. Inst. Min. Metal. Pet. Eng.*, **171**, 130 (1947).
103. K. N. Tu and U. Gosele, *Appl. Phys. Lett.*, **86**, 093111 (2005).
104. Y. D. Yin, R. M. Rioux, C. K. Erdonmez, S. Hughes, G. A. Somorjai and A. P. Alivisatos, *Science*, **304**, 711 (2004).
105. L. Dubau, J. Durst, F. Maillard, L. Guétaz, M. Chateneta, J. André and E. Rossinot, *Electrochim. Acta*, **56**, 10658 (2011).
106. L. Dubau, F. Maillard, M. Chatenet, L. Guetaz, J. André and E. Rossinot, *J. Electrochem. Soc.*, **157**, B1887 (2010).
107. F. Maillard, L. Dubau, J. Durst, M. Chatenet, J. André and E. Rossinot, *Electrochem. Commun.*, **12**, 1161 (2010).
108. L. Dubau, F. Maillard, M. Chatenet, J. André and E. Rossinot, *Electrochim. Acta*, **56**, 776 (2010).
109. C. H. Wang, C. Yang, Y. Y. Song, W. Gao and X. H. Xia, *Adv. Funct. Mater.*, **15**, 1267 (2005).
110. X. J. Chen, Y. Y. Wang, J. J. Zhou, W. Yan, X. H. Li and J. J. Zhu, *Anal. Chem.*, **80**, 2133 (2008).
111. D. Zhang, W. Gao, X. H. Xia and H. Y. Chen, *Chinese Sci. Bull.*, **51**, 19 (2006).
112. D. Zhang, Y. Ding, W. Gao, H. Y. Chen and X. H. Xia, *J. Nanosci. Nanotech.*, **8**, 979 (2008).
113. X. H. Li, L. Dai, Y. Liu, X. J. Chen, W. Yan, L. P. Jiang and J. J. Zhu, *Adv. Func. Mater.*, **19**, 3120 (2009).
114. L. Dai, L. P. Jiang, E. S. Abdel-Halim and J. J. Zhu, *Electrochem. Comm.*, **13**, 1525 (2011).
115. G. Madras and B. J. Coy, *Chem. Eng. Science*, **58**, 2903 (2003).
116. R. Nishida, P. Puengjinda, H. Nishino, K. Kakinuma, M. E. Brito, M. Watanabe and H. Uchida, *RSC Adv.*, **4**, 16260 (2014).
117. R. Nishida, K. Kakinuma, H. Nishino, T. Kamino, H. Yamashita, M. Watanabe and H. Uchida, *Solid State Ionics*, **180**, 968 (2009).
118. J. Li, J. Ren, G. Yang, P. Wang, H. Li, X. Sun, L. Chen, J. T. Ma and R. Li, *Mater. Sci. Eng. B*, **172**, 207 (2010).
119. Y. Hu, Q. Shao, P. Wu, H. Zhang and C. Cai, *Electrochem. Comm.*, **18**, 96 (2012).
120. X. W. Zhou, R. H. Zhang, Z. Y. Zhou and S. G. Sun, *J. Power Sources*, **196**, 5844 (2011).
121. G. Chen, D. Xia, Z. Nie, Z. Wang, L. Wang, L. Zhang and J. Zhang, *Chem. Mater.*, **19**, 1840 (2007).
122. O. A. Petrii, B. I. Podlovchenko, A. N. Frumkin and H. Lal, *J. Electroanal. Chem.*, **10**, 253 (1965).
123. V. S. Bagotzki and Y. Vassileiv, *Electrochim. Acta*, **12**, 1323 (1967).
124. X. H. Xia, T. Iwasita, F. Ge and W. Vielstich, *Electrochim. Acta*, **41**, 711 (1996).
125. T. Iwasita, *Electrochim. Acta*, **47**, 3663 (2002).
126. Y. N. Wu, S. J. Liao, Z. X. Liang, L. J. Yang and R. F. Wang, *J. Power Sources*, **194**, 805 (2009).
127. Y. Hu, P. Wu, Y. Yin, H. Zhang and C. X. Cai, *Appl. Cata. B: Env.*, **111**, 208 (2012).
128. J. Zhao, W. X. Chen, Y. F. Zheng and X. Li, *J. Power Sources*, **162**, 168 (2006).
129. S. J. Guo, Y. X. Fang, S. J. Dong and E. K. Wang, *J. Phys. Chem. C*, **111**, 17104 (2007).
130. A. N. Golikand, M. Asgari, M. G. Maragheh and S. Shahrokhian, *J. Electroanal. Chem.*, **588**, 155 (2006).
131. G. G. Wildgoose, F. G. Chevallier, L. Xiao, C. A. Thorogood, S. J. Wilkins, A. Crossley, L. Jiang, T. T. G. Jones, J. Jones and R. G. Compton, *J. Mater. Chem.*, **16**, 4103 (2006).
132. B. Børresen, G. Hagen and R. Tunold, *Electrochim. Acta*, **47**, 1819 (2002).
133. I. García, M. Torres, M. Crespo, C. Rodríguez and E. Estrada, *J. Alloy Comp.*, **434**, 764 (2007).
134. J. Hwang and J. Chung, *Electrochim. Acta*, **38**, 2715 (1993).
135. B. Hayden, D. Malevich and D. Pletcher, *Electrochem. Comm.*, **3**, 395 (2001).
136. E. Balko, *Stud. Inorg. Chem.*, **11**, 267 (1991).
137. M. A. Domínguez-Crespo, E. Ramírez-Meneses, A. M. Torres-Huerta, V. Garibay-Febles and K. Philippot, *Int. J. Hydrogen Energy*, **37**, 479 (2012).
138. R. Parsons, *Trans. Faraday Soc.*, **54**, 1053 (1958).
139. H. Kita, S. Ye and Y. Gao, *J. Electroanal. Chem.*, **334**, 351 (1992).
140. R. Gómez, A. Fernández-Vega, J. M. Felui and A. Aldaz, *J. Phys. Chem.*, **97**, 4769 (1993).
141. B. E. Conway, In: A. Wieckowski, editor. Interfacial electrochemistry: theory, experiment, and applications, New York, Marcel Dekker, 131 (1999).
142. T. Nishimura, T. Morikawa, M. Yokoi, C. Iwakura and H. Inoue, *Electrochim. Acta*, **54**, 499 (2008).
143. Q. Z. Jiang, X. Wu, M. Shen, Z. F. Ma and X. Y. Zhu, *Catal. Lett.*, **124**, 434 (2008).
144. I. Savych, B. d'Arbigny, S. Subianto, S. Cavaliere, D. J. Jones and J. Rozière, *J. Power Sources*, **257**, 147 (2014).

145. V. Alves, L. Silva, E. Oliveira and J. Boodts, *Mater. Sci. Forum*, **289**, 655 (1998).
146. X. Chen, G. Chen and P. Yue, *J. Phys. Chem. B*, **105**, 4623 (2001).
147. V. Alves, L. Silva, J. Boodts and S. Trasatti, *Electrochim. Acta*, **27**, 1585 (1994).
148. A. Czerwinski, R. Marassi and S. Zamponi, *J. Electroanal. Chem.*, **316**, 211 (1991).
149. R. Woods, In: A. Bard, Editor, *Chemisorption at electrodes in electroanalytical chemistry*, New York, Marcel Dekker, **9** (1976).
150. A. Czerwinski, *J. Electroanal. Chem.*, **379**, 487 (1994).
151. A. Czerwinski, R. Marassi and S. Zamponi, *J. Electroanal. Chem.*, **316**, 211 (1991).
152. U. Diebold, *Surf. Sci. Rep.*, **48**, 53 (2003).
153. G. A. Niklasson and C. G. Granqvist, *J. Mater. Chem.*, **17**, 127 (2007).
154. D. R. Lide, CRC handbook of chemistry and physics, 73rd Ed. CRC Press, Boca Raton, FL (2000).
155. P. Lunkenheimer, A. Loidl, C. R. Ottermann and K. Bange, *Phys. Rev. B*, **44**, 5927 (1991).
156. Y. G. Yoon, G. G. Park, T. H. Yang, J. N. Han, W. Y. Lee and C. S. Kim, *Int. J. Hydrogen Energy*, **28**, 657 (2003).
157. I. Radev, E. Slavcheva and E. Budevski, *Int. J. Hydrogen Energy*, **32**, 872 (2007).